Inorg. Chem. **2008**, *47*, 5129−5135

Nitrogen-Ligated Iron Complexes: Photolytic Approach to the FeN^+ Moiety

Drew Buschhorn, Maren Pink, Hongjun Fan, and Kenneth G. Caulton*

Department of Chemistry, Indiana University, Bloomington, Indiana 47405

Received November 21, 2007

The synthesis of (PNP)FeCl, (PNP)Fe[NH(xylyl)], and (PNP)FeN_3 are reported(PNP = $(^tBu_2PCH_2SiMe_2)_2N^-$). While the azide is thermally stable, it is photosensitive to lose N_2 and form $[(PNP{=}N)Fe]_2$,in which the nitride ligand has formed a double bond to one phosphorus, and this N bridges to a second iron to form a 2-fold symmetric dimer. The reaction energy to form the (undetected) monomeric $[\eta^3$-$^tBu_2PCH_2SiMe_2NSiMe_2CH_2P^tBu_2{=}N]Fe$ is −15.9 kcal/mol, so this $P^{III} \rightarrow P^V$ oxidation is favorable. The η^2 version of this same species is less stable by 23.7 kcal/mol, which shows that the loss of one P→ Fe bond is caused by dimerization, and therefore, it does not precede and cause dimerization. A comparison is made to Ru analogs.

Introduction

We reported earlier[1] that reactions designed to produce (PNP)Ru(N_3), PNP = $(^tBu_2PCH_2SiMe_2)_2N^-$, proceed with rapid loss of N_2 to deliver (PNP)RuN, a (slightly) nonplanar molecule with a multiple Ru/N bond containing d^4-Ru^{IV}. This molecule is persistent at 25 °C for days, both in benzene solution and in the solid state. We report here results that enable evaluation of periodic trends up Group 8B by describing the analogous iron chemistry. Iron chemistry of imide and nitride ligands has experienced considerable recent study,[2–9] including one puzzling report,[10] showing how an FeN^+ unit is thermodynamically fated to form $FeNNFe^{2+}$; these last results were established with a C_3 symmetric anionic tripodal tris-phosphine borate ligand. Of special interest to us in this class of compounds is to establish both the intrinsic Fe/E bond character (single, double, electrophilic, nucleophilic), as well as its reactivity, for E = N versus E = O. Oxidative utilization of high-valent FeO^{q+} is of both biological and catalytic relevance.[11,12] If an FeN unit can oxidize H_2, this would be one step in the hydrogenation[13] of N_2: nitrogen fixation. Our FeN^+ results, reported here, are set in the above 2-fold-symmetric PNP environment whose π donor strength is established[14] to be considerable.

Results

Synthesis of (PNP)FeCl. The reaction of equimolar (PNP)MgCl with anhydrous $FeCl_2$ in THF resulted in a clean conversion to (PNP)FeCl. The ^1H NMR spectrum (Figure 1) shows that (PNP)FeCl appears to be C_{2v} symmetric in solution, with three broad signals for the CH_2, Si−Me, and P−^{t}butyl peaks. A ^{31}P NMR spectrum shows no signal in a wide window suggesting that the phosphorus atoms are directly bound to a paramagnetic iron center. A magnetic moment determination (Evans method) was performed and confirmed the complex to be high spin ($\mu_{eff} = 4.6\ \mu_B$) with four unpaired electrons. A crystal structure determination

* To whom correspondence should be addressed. E-mail: caulton@indiana.edu.

(1) Walstrom, A.; Pink, M.; Yang, X.; Tomaszewski, J.; Baik, M.-H.; Caulton, K. G. *J. Am. Chem. Soc.* **2005**, *127*, 5330.
(2) Sadique, A. R.; Gregory, E. A.; Brennessel, W. W.; Holland, P. L. *J. Am. Chem. Soc.* **2007**, *129*, 8112.
(3) Eckert, N. A.; Vaddadi, S.; Stoian, S.; Lachicotte, R. J.; Cundari, T. R.; Holland, P. L. *Angew. Chem., Int. Ed.* **2006**, *45*, 6868.
(4) Stoian, S. A.; Vela, J.; Smith, J. M.; Sadique, A. R.; Holland, P. L.; Muenck, E.; Bominaar, E. L. *J. Am. Chem. Soc.* **2006**, *128*, 10181.
(5) Smith, J. M.; Lachicotte, R. J.; Pittard, K. A.; Cundari, T. R.; Lukat-Rodgers, G.; Rodgers, K. R.; Holland, P. L. *J. Am. Chem. Soc.* **2001**, *123*, 9222.
(6) Mankad, N. P.; Whited, M. T.; Peters, J. C. *Angew. Chem., Int. Ed.* **2007**, *46*, 5768.
(7) Rohde, J.-U.; Betley, T. A.; Jackson, T. A.; Saouma, C. T.; Peters, J. C.; Que, L., Jr. *Inorg. Chem.,* **2007**, *46*, 5720.
(8) Hendrich, M. P.; Gunderson, W.; Behan, R. K.; Green, M. T.; Mehn, M. P.; Betley, T. A.; Lu, C. C.; Peters, J. C. *Proc. Natl. Acad. Sci. U. S. A.* **2006**, *103*, 17107.
(9) Thomas, C. M.; Mankad, N. P.; Peters, J. C. *J. Am. Chem. Soc.* **2006**, *128*, 4956.
(10) Betley, T. A.; Peters, J. C. *J. Am. Chem. Soc.* **2004**, *126*, 6252.
(11) Costas, M.; Mehn, M. P.; Jensen, M. P.; Que, L., Jr. *Chem. Rev.,* **2004**, *104*, 939.
(12) Shaik, S.; Hirao, H.; Kumar, D. *Acc. Chem. Res.* **2007**, *40*, 532.
(13) Brown, S. D.; Mehn, M. P.; Peters, J. C. *J. Am. Chem. Soc.* **2005**, *127*, 13146.
(14) Ingleson, M. J.; Pink, M.; Caulton, K. G. *J. Am. Chem. Soc.* **2006**, *128*, 4248.

10.1021/ic702279b CCC: $40.75
Published on Web 05/15/2008

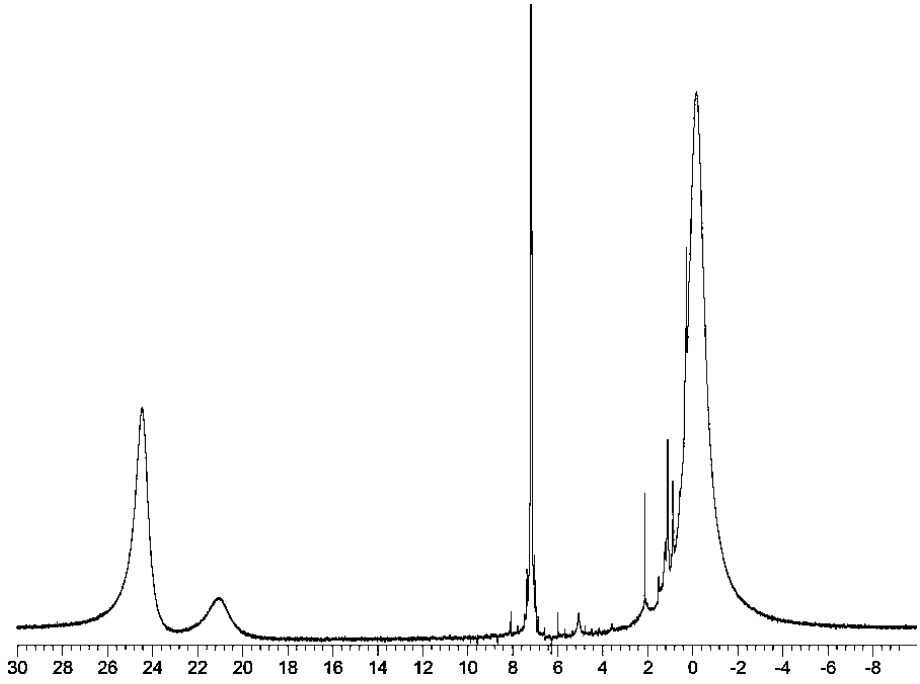

Figure 1. ^{1}H NMR spectrum (300 MHz) of [(^{t}Bu$_2$PCH$_2$SiMe$_2$)$_2$N]FeCl in C_6D_6(trace C_6D_5H at 7.15 ppm) at 20 °C. ^{t}Bu: −0.8 ppm. SiMe: 24 ppm.

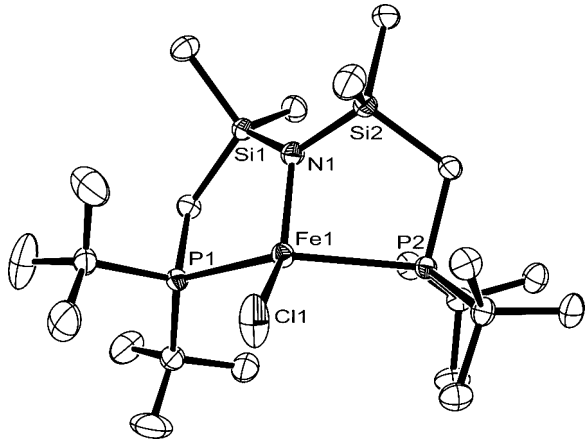

Figure 2. ORTEP drawing (50% probabilities) of the non-hydrogen atoms of [(^{t}Bu$_2$PCH$_2$SiMe$_2$)$_2$N]FeCl. Unlabeled atoms are carbon. Selected structural parameters: Fe1−N1 = 1.9824(18) Å, Fe1−Cl1 = 2.2708(7) Å, Fe1−P1 = 2.4943(6) Å, Fe1−P2 = 2.5824(6) Å, N1−Fe1−Cl1 = 139.98(6)°, N1−Fe1−P1 = 92.50(5)°, Cl1−Fe1−P1 = 103.59(2)°, N1−Fe1−P2 = 88.22(5)°, Cl1−Fe1−P2 = 103.01(2)°, P1−Fe1−P2 =137.07(2)°.

(Figure 2) shows a monomeric four-coordinate nonplanar structure around iron.[15] Because this is, at best, C_s symmetric, the higher symmetry observed in the ^{1}H NMR spectrum implies that the chloride rapidly flexes above and below the P−N−P plane in solution (inverting the geometry at iron), resulting in the observed spectrum being time-averaged to C_{2v} symmetry. The molecule has significantly (by 0.1 Å) inequivalent Fe/P distances, apparently caused by the different ring conformations of the two fused rings of the coordinated pincer. All distances to iron are long enough to be consistent with a high-spin Fe^{II}. The Fryzuk group has reported (PNP^{Ph})FeX with X = Cl and CH(SiMe$_3$)$_2$ when the PNP^{Ph} ligand contains phenyl substituents on P. These are both $S = 2$ systems and, thus, are nonplanar.[16]

(PNP)FeCl shows no reaction in benzene in the presence of (equimolar) N_2, H_2, or CO.

Synthesis of (PNP)Fe(N$_3$). Reaction of (PNP)FeCl with excess NaN_3 in THF gives conversion to (PNP)Fe(N$_3$), characterized by ^{1}H NMR and also by infrared spectroscopy(azide band at 2073 cm^{-1}). While the solid is nearly colorless, benzene solutions are dark yellow. The ^{1}H NMR spectrum of (PNP)Fe(N$_3$) shows time-averaged C_{2v} symmetry, with one signal each for ^{t}Bu and for SiMe groups. Its chemical shifts are readily distinguished from those of the chloride, so that any chloride impurity can be readily detected in the azide.

Crystals grown from pentane show (Figure 3) a nonplanar coordination geometry with transoid angles from 131° to 136° and a bent bonding of azide to Fe (Fe−N2−N3 = 137°). The two Fe/P distances differ only modestly, by 0.06 Å, perhaps because of the different conformations of the two fused 5-membered rings of the pincer (angles P−Fe−N1 = 89° and 94°). The Fe/N distances differ negligibly. The FeN$_3$ group is oriented to minimize any contacts with the four ^{t}Bu groups.

Toward a Nitride Complex. (a) Synthesis and Characterization. Photolysis[17–19] of this azide complex in benzene gives rapid evolution of gas, with darkening, to give a product whose ^{1}H NMR spectrum shows two signals each for ^{t}Bu, SiMe, and CH$_2$. The ^{31}P NMR spectrum of this

(15) Renkema, K. B.; Ogasawara, M.; Streib, W. E.; Huffman, J. C.; Caulton, K. G. *Inorg. Chim. Acta* **1999**, *291*, 226.

(16) Fryzuk, M. D.; Leznoff, D. B.; Ma, E. S. F.; Rettig, S. J.; Young, V. G., Jr. *Organometallics,* **1998**, *17*, 2313.

(17) Berry, J. F.; Bill, E.; Bothe, E.; George, S. D.; Mienert, B.; Neese, F.; Wieghardt, K. *Science,* **2006**, *312*, 1937.

(18) Aliaga-Alcalde, N.; George, S. D.; Mienert, B.; Bill, E.; Wieghardt, K.; Neese, F. *Angew. Chem., Int. Ed.* **2005**, *44*, 2908.

(19) Petrenko, T.; DeBeer George, S.; Aliaga-Alcalde, N.; Bill, E.; Mienert, B.; Xiao, Y.; Guo, Y.; Sturhahn, W.; Cramer, S. P.; Wieghardt, K.; Neese, F. *J. Am. Chem. Soc.* **2007**, *129*, 11053.

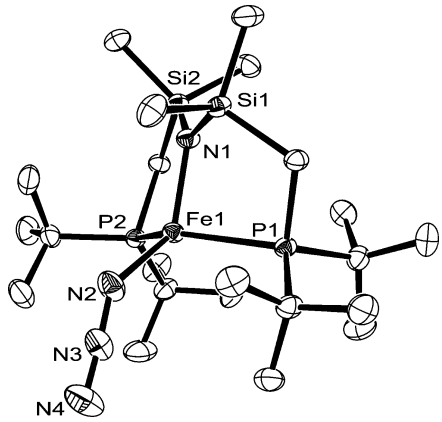

Figure 3. ORTEP view (50% probabilities) of the non-hydrogen atoms of (PNP)Fe(N_3). Unlabeled atoms are carbon. Selected structural parameters: Fe1−N2 = 1.9613(14) Å, Fe1−N1 = 1.9691(12) Å, Fe1−P2 = 2.4878(4) Å, Fe1−P1 = 2.5503(4) Å, N2−N3 = 1.191(2) Å, N3−N4 = 1.151(2) Å, N2−Fe1−N1 = 131.00(6)°, N2−Fe1−P2 = 106.28(5)°, N1−Fe1−P2 = 94.16(4)°, N2−Fe1−P1 = 103.66(5)°, N1−Fe1−P1 = 89.46(4)°, P2−Fe1−P1 = 136.333(15)°, N3−N2−Fe1 = 137.46(14)°, N4−N3−N2 = 175.9(2)°.

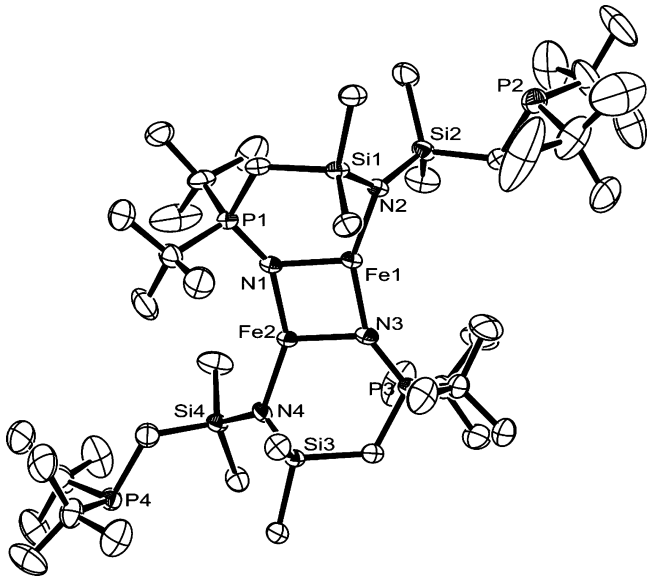

Figure 4. ORTEP view (50% probabilities) of the non-hydrogen atoms of the general position dimer [(PNP═N)Fe]$_2$. Unlabeled atoms are carbon. Selected structural parameters: Fe1−N3 = 1.895(4) Å, Fe1−N2 = 1.936(4) Å, Fe1−N1 = 1.946(4) Å, Fe1−Fe2 = 2.5417(10) Å, Fe2−N1 = 1.908(4) Å, Fe2−N4 = 1.939(4) Å, Fe2−N3 = 1.943(4) Å, P1−N1 = 1.578(4) Å, P3−N3 = 1.587(4) Å, N3−Fe1−N2 = 148.42(18)°, N3−Fe1−N1 = 97.26(17)°, N2−Fe1−N1 = 112.85(17)°, N1−Fe2−N4 = 149.19(18)°, N1−Fe2−N3 = 96.92(17)°, N4−Fe2−N3 = 112.61(17)°.

product shows no signal, consistent with line broadening from rapid paramagnetic relaxation. Together these NMR data indicate that the product is not a singlet state and is not C_{2v} symmetric. Crystals grown from pentane were shown (Figure 4) to contain the expected two nitrogens per Fe but in a dimeric structure and with formation of one imine P═N bond for each Fe.[20] One arm of each former pincer ligand is pendant, leaving each iron three coordinate. A nitrogen ligand has coupled with trivalent phosphorus. Because P is oxidized by two electrons, the iron oxidation state remains unchanged at +2. The asymmetric unit of the unit cell contains one full dimer and one-half dimer, the latter possessing a crystallographic center of symmetry. There are no significant differences in bond lengths or angles between the two dimers. Even the dimer in the general position in the asymmetric unit has an idealized C_2 axis relating the two ends of the molecule. The three coordinate geometry at iron is distorted toward T-shaped; this probably reflects what would be steric interference between the bridging N═P^{t}Bu$_2$ group and the P^{t}Bu$_2$ group, which is pendant, because that is the largest angle around Fe. The dimer is planar (within 2°) at both metals and at both phosphiniminate nitrogens. All three Fe/N distances to a given iron are equal to within ±0.02 Å, and the P/N distances are short, consistent with a multiple bond.[21] Both 2-fold-symmetric Fe_2N_2 quadrangles have their shorter Fe/N distances to the iron to which that N is not chelated. The Fe/Fe distance, ∼2.55 Å, is comparable to that in other related compounds.[22] The larger N−Fe−N angle, ∼149° (vs 112°), is nevertheless apparently not suitable for binding the bulky P^{t}Bu$_2$ donor of the pendant arm. The 6-membered ring formed by the coordinated pincer arm is highly nonplanar, which twists the amide plane unusually far from the iron coordination plane, an effect unusual in η^3-pincer structures. However, if ring torsions have only a modest barrier; then the dimer will have a time-averaged mirror plane of symmetry containing the Fe_2N_2 quadrangle, hence the observed equivalence of both ^{t}Bu and Me groups on a given P or Si. This easy flexibility is consistent with the fact that the half-dimer has rigorous inversion symmetry, hence a different conformation from the whole dimer in the asymmetric unit (idealized C_2 symmetry).

(b) Energetics and Mechanism. Why is this product formed? We have addressed some aspects of this question by DFT(PBE) calculation of both an anticipated primary product, (PNP)FeN, and also the monomeric part of the dimer, (PNP═N)Fe, the latter with the ligand bound both η^2 and η^3. We have calculated both singlet and triplet states for all these species.

There are two general classes of mechanism, distinguished by the timing of P/N bond formation versus dimerization events: which occurs first? If P/N bonding occurs first, it could either be a migration of coordinated P to N or first dissociation to form one free P arm, then unimolecular attack on the local N. The fact that we find very inequivalent Fe/P bond lengths in both the chloride and the anilide reported here (below) indicates that it might be generally possible to dissociate one phosphine arm. If this dissociation of one P arm begins the reaction, then this nucleophilic P could also attack N on a different iron, to start dimerization concurrent with P/N bond formation. However our past reasoning in (PNP)M chemistry has generally been that the steric protection conferred by the PNP ligand prevents reactions bimo-

(20) LePichon, L.; Stephan, D. W.; Gao, X.; Wang, Q. *Organometallics* **2002**, *21*, 1362.

(21) Dehnicke, K.; Straehle, J. *Polyhedron* **1989**, *8*, 707.

(22) Olmstead, M. M.; Power, P. P.; Shoner, S. C. *Inorg. Chem.* **1991**, *30*, 2547.

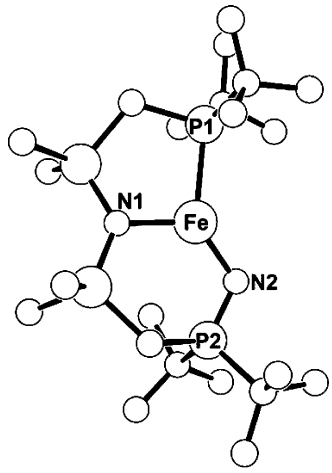

Figure 5. DFT-optimized structure of (PNP═N)Fe; only the non-hydrogen atoms are shown.

lecular in complex.[13,23] Thus, we focused our DFT(PBE) calculation on the two unimolecular mechanisms; all quoted energies are electronic energies.

We found minima for both singlet and triplet (PNP)FeN, with the singlet more stable by 14.5 kcal/mol. The reaction energies for conversion of (PNP)Fe(N_3), which is calculated to have a quintet ground state, to singlet (PNP)FeN + N_2 is −4.7 kcal/mol, thus favorable, but only modestly so. However, the reaction energy for singlet (PNP)FeN to isomerize to (PNP═N)Fe (Figure 5), the monomer of the observed dimer, is −11.2 kcal/mol. The iron in this three-coordinate product (Figure 5) is divalent, and this species is again found to have a quintet ground state. Thus, the overall reaction for monomeric iron species is favorable, and the last step in particular, reduction of Fe^{IV} to Fe^{II}, as phosphorus is oxidized from +3 to +5, drives the reaction.

This P/N bond formation might occur if the nitrogen is oxidizing, as it is in RN_3.[21] Singlet (PNP)FeN was therefore analyzed for such character at N or in the FeN unit. The calculated Fe/N distance to the nitride is 1.52 Å and, thus, is consistent with a triple bond; for comparison, the Fe/NSi_2 distance is 1.94 Å. Three orbitals in Figure 6 comprise the Fe−N σ and an orthogonal pair of π bonds. The three highest-energy occupied orbitals (see Supporting Information) are two primarily d orbitals (hence d^4-Fe^{IV}) and a lone pair mainly on the amide nitrogen(HOMO−2).

The character of the Fe/nitride bond is also revealed by comparison to the geometric and electronic structure of the triplet state of (PNP)FeN. As shown in Table 1, the Fe/N distance to nitride (N2) is longer in the triplet (as are all other metal/ligand bonds). The triplet spin densities are mainly on iron(1.89e), with only 0.04 on amide N and 0.11 on nitride N. Two Fe/N π bonding orbitals can be identified (Figure 6), but SOMO1 is π^*_{FeN}, thus reducing the FeN bond order below 3. It is the two SOMOs that give the (modest) spin density on nitride N, yet the nitride reacts as an oxidant. Therefore, the favorable thermodynamics for P═N bond formation is not determined simply by ground-state character of the reagent nitride nitrogen and not by one or two frontier orbitals but rather by more general reaction characteristics, including those of the product.

Fe/P dissociation prior to oxidation of phosphorus encounters an energy cost to form the stationary state singlet (η^2-PNP)FeN of +23.0 kcal/mol. While not impossible, this is probably inconsistent with the rapid rate of our reaction (at 25 °C in a water-cooled photochemical reactor). The reaction certainly does not proceed via an excited state because thermalization/decay to ground electronic state would have occurred long before this stage is reached (i.e., soon after N_2 loss). We therefore favor a unimolecular migration/insertion for forming the P/N bond: P/N bond formation concurrent with Fe/P bond scission.

Synthesis of (PNP)Fe[NH(xylyl)]. Anilide ligands serve to evaluate the interaction of a metal center with a reduced form of nitrogen.[24–26] The title molecule was rapidly formed by reaction of equimolar LiNH(xylyl) with (PNP)FeCl in benzene. The structure of a light brown crystal grown from pentane (Figure 7) shows a nonplanar coordination geometry. The hydrogen found in the difference Fourier map confirms that the molecule is an anilide, not an imide. The nonplanarity at iron is best seen in the two trans angles, PFeP at 138.128(17)° and NFeN at 127.08(6)°. The distance from iron to the anilide N is only slightly (0.04 Å) shorter than that to the silylamide N; this distance falls in the range (1.92−1.94Å) of other 4-coordinate Fe^{II} anilides.[27–29] The Fe−N2−C_{ipso} angle of 141.01(12)° is not characteristic of an imide. The molecule has no agostic interactions to any methyl (shortest distance to a ^{t}Bu or SiMe carbon is 3.71 Å and to xylyl methyl is 3.31 Å). An unusual feature of the coordination geometry is that the two Fe/P distances differ dramatically (by 0.1 Å) with the longer distance being to P1, which is part of the highly nonplanar five-membered chelate ring; this may be diagnostic of strain because the other pincer ring is nearly planar. Without this distortion, which leaves the two nonbonded P/N2 distances equal within 0.06 Å, one such contact might be destabilizing. The angles from anilide N to P are identical (106°). The silylamide nitrogen nevertheless remains planar in this pincer conformation. This ferrous complex is crystallographically isomorphous with its Co^{II} analog.[30] M−P and M−N(xylyl) distances are shorter for M = Co.

A least-squares fit[31] of the structures of (PNP)FeCl to that of (PNP)Fe(N_3) shows them to be extremely similar, even to the conformation around single bonds. The anilide is more

(23) Indeed our DFT search for bimolecular intermediates here led only to separation of the two halves during geometry optimization.

(24) Brown, S. D.; Peters, J. C. *J. Am. Chem. Soc.* **2004**, *126*, 4538.
(25) Betley, T. A.; Peters, J. C. *J. Am. Chem. Soc.* **2003**, *125*, 10782.
(26) Brown, S. D.; Betley, T. A.; Peters, J. C. *J. Am. Chem. Soc.* **2003**, *125*, 322.
(27) Eckert, N. A.; Smith, J. M.; Lachicotte, R. J.; Holland, P. L. *Inorg. Chem.* **2004**, *43*, 3306.
(28) Au-Yeung, H. Y.; Lam, C. H.; Lam, C.-K.; Wong, W.-Y.; Lee, H. K. *Inorg. Chem.* **2007**, *46*, 7695.
(29) Stokes, S. L.; Davis, W. M.; Odom, A. L.; Cummins, C. C. *Organometallics* **1996**, *15*, 4521.
(30) Ingleson, M. J.; Pink, M.; Fan, H.; Caulton, K. G. *Inorg. Chem.* **2007**, *46*, 10321.
(31) See Supporting Information.

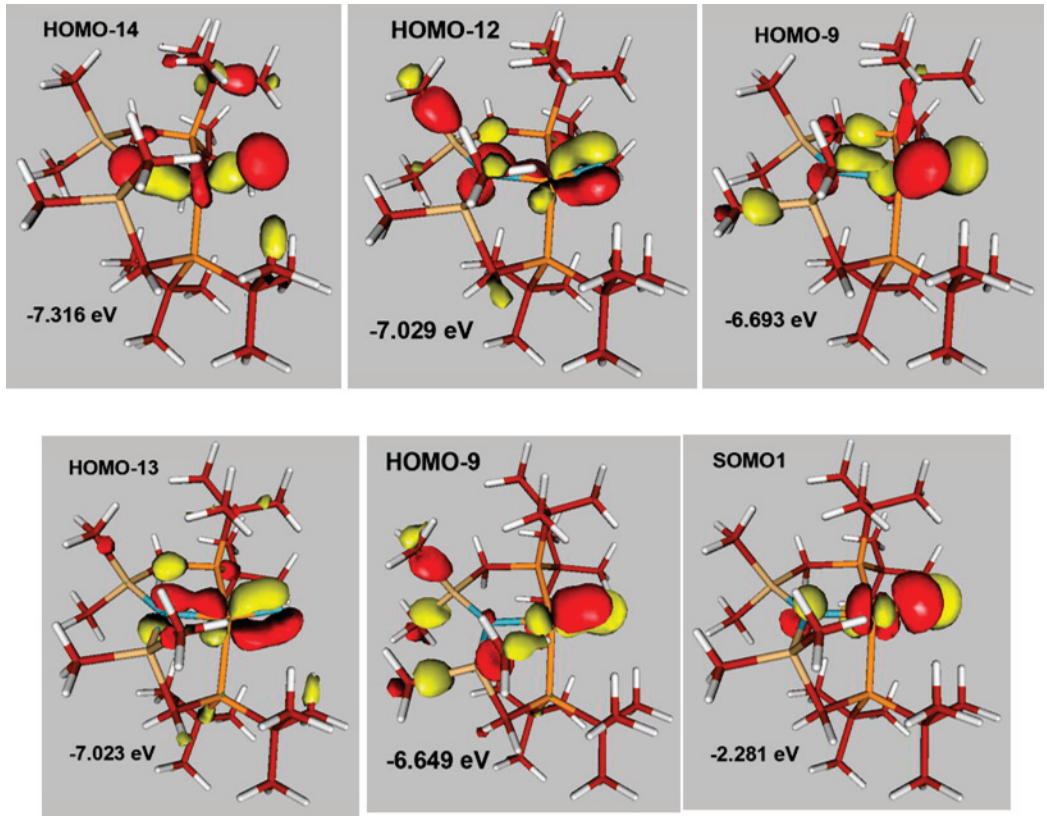

Figure 6. Selected frontier orbitals of singlet (upper) and triplet (lower) (PNP)FeN.

Table 1. Selected Bond Lengths (Å) and Angles (deg) of (PNP)FeN

singlet		triplet	
Fe−P1	2.271	Fe−P1	2.287
Fe−P2	2.302	Fe−P2	2.432
Fe−N1	1.938	Fe−N1	2.050
Fe−N2	1.524	Fe−N2	1.586
P1−Fe−P2	141.4	P1−Fe−P2	138.4
N1−Fe−N2	134.5	N1−Fe−N2	156.3

different from the chloride, specifically concerning the pincer ring conformations. For all three structures, the Fe−NSi2 distances are unexceptional.[16,22,32,33]

The ^{1}H NMR spectrum of (PNP)Fe[NH(xylyl)] in benzene shows one signal each for ^{t}Bu, SiMe, and CH_2 protons, suggesting C_{2v} symmetry by time-averaged inversion of the nonplanar Fe coordination geometry. However, the 2,6-xylyl protons show inequivalent methyl signals and inequivalent meta protons(as well as one *para* proton signal), suggesting slow rotation around the N−C_{ipso} bond, even as the iron inverts rapidly. This shows how the planar anilide is hindered by the four flanking ^{t}Bu groups, as was the Fe/azide group.

Discussion

The apparent attack here of phosphorus on a nitride ligand has some relation to chemistry we have reported[34] for (PNP)Co(N_3), which itself has one more electron than the iron species reported here, and which is recovered unchanged after 4 days reflux in benzene. Indeed, to elicit (thermal) reactivity, it was necessary to first do one-electron outer sphere oxidation (with ferricinium) of this Co^{II} species, and then (PNP)Co(N_3)$^+$ rapidly evolved N_2. As with the iron case here, the product detected at 25 °C is not a terminal nitride (Figure 8). However, the oxidation product (PNP)CoN$^+$, now isoelectronic with the Fe case, showed reactivity even beyond that shown by the isoelectronic Fe analog: "deeper" ligand

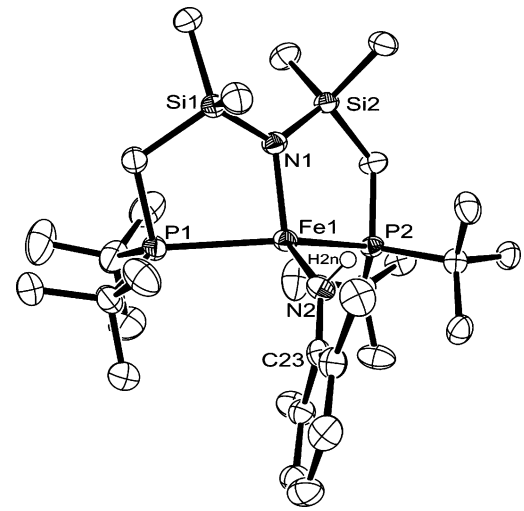

Figure 7. ORTEP view (50% probabilities) of (PNP)Fe[NH(xylyl)]. Only the hydrogen on the anilide nitrogen is illustrated. Unlabeled atoms are carbon. Selected structural parameters: Fe1−N2 = 1.9505(15) Å, Fe1−N1 = 1.9893(14) Å, Fe1−P2 = 2.5480(5) Å, Fe1−P1 = 2.6336(5) Å, N2−Fe1−N1 = 127.08(6)°, N2−Fe1−P2 = 107.03(5) Å, N1−Fe1−P2 = 92.50(4) Å, N2−Fe1−P1 = 106.23(5) Å, N1−Fe1−P1 = 87.23(4) Å, P2−Fe1−P1 = 138.128(17) Å, C23−N2−Fe1 = 141.01(12) Å.

(32) Andersen, R. A.; Faegri, K.,Jr.; Green, J. C.; Haaland, A.; Lappert, M. F.; Leung, W. P.; Rypdal, K. *Inorg. Chem.* **1988**, *27*, 1782.
(33) Panda, A.; Stender, M.; Olmstead, M. M.; Klavins, P.; Power, P. P. *Polyhedron* **2003**, *22*, 67.
(34) Ingleson, M. J.; Pink, M.; Fan, H.; Caulton, K. G. *J. Am. Chem. Soc.* **2008**, *130*, 4262.

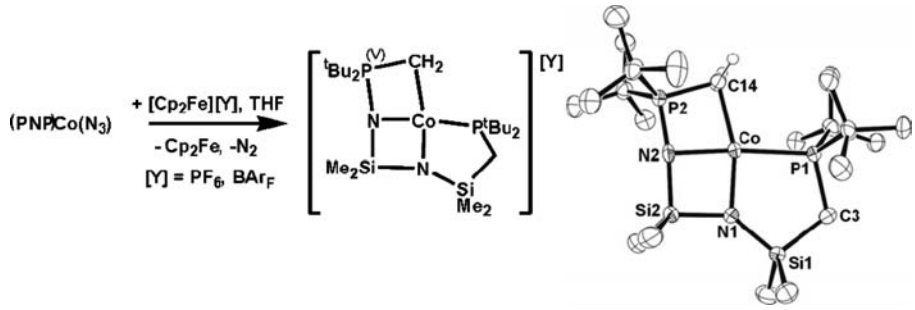

Figure 8. Schematic and ORTEP view (50% probabilities) of the cationic product from outer sphere oxidation of (PNP)Co(N$_3$).

rearrangement. Thus, although a P/N bond was formed, this was accompanied by reversal of the Si−C and Si−N bonds, to give two small rings. This is obviously a way to keep coordination number four for P, and to minimize ^{t}Bu repulsions but avoid the entropy penalty of dimerization which characterizes the iron analog. A feature shared by Fe and Co is that one M/P bond is lost by double bonding to the nitride. In sum, the isoelectronic cationic analog for cobalt takes a different course, giving a product with wholly different connectivity than the iron case. This difference is perhaps a result of the higher charge in the cobalt case (more electrophilic metal center), together with a consequent higher need of cobalt to be four coordinate. For example, the higher charge of Co^{III} may prevent loss of phosphorus donor subsequent to P═N bond formation, hence preventing dimerization from a crowded 3-coordinate species (PNP═N)Co$^+$. The longer lifetime of this monomeric species then permits intramolecular N attack on Si, leading to the observed cobalt product. The unfavorable Coulomb factor for dimerization of two cations will also lengthen the lifetime of the cobalt monomer. Support for this idea comes from DFT calculation of the energy for dissociation of the ^{t}Bu$_2$P arm from (PNP═N)Fe versus (PNP═N)Co$^+$. For iron, the energy is 23.7 kcal/mol (both complexes are quintet ground states), while for (PNP═N)Co$^+$ the energy is 29.4 kcal/mol (here both are triplets).

The expulsion of N_2 is a highly selectively photochemical event because heating a solution of (PNP)Fe(N$_3$) for 48 h at 80 °C in toluene returned only unreacted starting material. Indeed, the thermal stability is noteworthy and consistent with the large number of azide complexes studied recently for their magnetic properties.[35,36] This thermal stability is especially interesting because[21] the thermal Staudinger reaction converts free phosphine and azide R′N$_3$ to R$_3$P = N$_3$R′; the fact that **A** does not form upon heating (PNP)Fe(N$_3$) indicates that binding to Fe^{II} suppresses this reaction, even if a "phosphine arm-off" species is thermally accessible.

Comparison to the ruthenium analog[1] is informative of periodic trends based on the DFT calculations. Why are the products different for iron versus ruthenium? Loss of N_2 from (PNP)M(N$_3$) is calculated to be about 16 kcal/mol more favorable for M = Ru than it is for iron, consistent with the heavier divalent analog being more reducing (i.e., the heavier metal favoring more its higher oxidation state). For the P═N bond formation, this reaction is about 37 kcal/mol more favorable for iron, consistent with this reduction of metal being favored for the lighter metal. Indeed the reaction energy for formation of (PNP═N)Ru from its nitride isomer is +25.6 kcal/mol, so will not occur; this is consistent with experiment in that (PNP)RuN is persistent for days in solution at 25 °C.

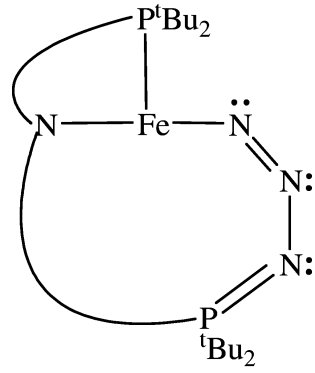

A

Another example of P═N bond formation has been reported, for P on a tantalum nitride, where free phosphorus is less likely.[37] This is a case, contrasting to ours for Ru, where even a 5d metal is reduced rather than adopt the Ta^V state with N^{3-}.

It is also interesting that (PNP)Fe[NH(xylyl)] is not a singlet ground state(based on NMR spectra), given that there is π donation from both silylamide and anilide lone pairs, which might have forced spin pairing. Apparently neither of these is a sufficiently strong π-donor to separate the d orbitals enough to overcome the spin pairing energy in this low coordination number and quasi-tetrahedral ligand field. Hence two strong π bonds are needed to cause spin pairing.

The work described shows that intramolecular capture of a presumed FeN$^+$ unit is the favored reaction channel. While this represents loss of the reactive monatomic ligand for bimolecular use, it does serve to define its high reactivity. Intramolecular capture is increasingly the fate of later 3d metalloligand multiple bonds in high oxidation states. In general, ligand vulnerabilities (here phosphorus is more reducing than iron) set limits on this metal/O or metal/N chemistry, but every ligand has its specific vulnerability,[37–41]

(35) Ribas, J.; Escuer, A.; Monfort, M.; Vicente, R.; Cortes, R.; Lezama, L.; Rojo, T. *Coord. Chem. Rev.* **1999**, 1027.
(36) Escuer, A.; Aromi, G. *Eur. J. Inorg. Chem.* **2006**, 472.
(37) Spencer, L. P.; MacKay, B. A.; Patrick, B. O.; Fryzuk, M. D. *Proc. Natl. Acad. Sci. U. S. A.* **2006**, *103*, 17094.
(38) Morello, L.; Yu, P.; Carmichael, C. D.; Patrick, B. O.; Fryzuk, M. D. *J. Am. Chem. Soc.* **2005**, *127*, 12796.

and diminishing the oxidizability of the ligand donor atom is required based on the results reported here.

Experimental Section

General Considerations: Standard techniques for inert atmosphere (argon) conditions were used for air-sensitive manipulations. All solvents, including deuterated NMR solvents, were dried and stored under argon. ^{1}H and ^{31}P NMR spectra were recorded on Varian spectrometers, either a Gemini XL300 or a Unity I400 instrument, with chemical shifts reported in parts per million and referenced to each specific solvent, with the exception of ^{31}P which was externally referenced to H_3PO_4 (neat). No ^{31}P NMR signal was observed for any of the paramagnetic species reported here. All IR values reported were taken in a 0.1 mm path length KBr gastight solution cell dissolved in pentane or as solids. Because these new compounds are very soluble and resist crystallization, product homogeneity is supported by NMR spectra in the Supporting Information. In multiple executions, the progress of each reaction over time was monitored by multinuclear NMR spectroscopy, and yields are essentially quantitative, unless indicated otherwise. Mass spectra were determined on a Thermo Electron Corporation MAT 95XP-Trap mass spectrometer. In a nitrogen atmosphere glovebox, a solution in pentane was applied to the tungsten filament and dried. The filament was then quickly introduced into the instrument vacuum chamber and heated to approximately 400 °C.

(PNP)FeCl. Commercial anhydrous $FeCl_2$ (s) was heated at 120 °C for two days under vacuum and then allowed to cool overnight under vacuum. IR analysis was performed on the $FeCl_2$ in a Nujol mull to verify that no water was present. $FeCl_2$ (0.045 g, 0.35 mmol) was reacted with 0.200 g of (PNP)MgCl·dioxane (0.34 mmol) in 30 mL of dry THF. The heterogeneous mixture was stirred overnight resulting in a homogeneous clear yellow-brown solution. This was dried under vacuum, dissolved in a minimal amount of toluene, and filtered through a coarse frit. The resulting deep yellow-brown filtrate was dried slowly, then dissolved in 5 mL of pentane and filtered using a fine frit filter. The clear deep yellow filtrate was collected, concentrated to approximately 1 mL, and placed into a −40 °C freezer overnight. After 12 h, purple and colorless crystals totaling approximately 0.025 g (0.046 mmol) were collected for a 13% yield. The best of each color type were set aside for X-ray analysis as detailed below. The two color sets of crystals were shown to have the same composition, with the varying colors the result of dichroism. ^{1}H NMR (C_6D_6): δ 24 (br s, 12H, Si−CH_3), 21 (br s, 4H, P−CH_2-Si), −0.8 (br s, 36H, ^{t}butyl). ^{31}P NMR (C_6D_6): no signal. Evans method magnetic susceptibility:[31] μ_{eff} = 4.6 μ_B in C_6D_6. MS (positive ion methane CI): calcd (PNP)FeCl ($C_{22}H_{52}ClFeNP_2Si_2$), calcd 540.080 g/mol; obsd M^+ with correct isotopic abundances for one Cl.

(PNP)FeN_3. (PNP)FeCl (0.030 g, 0.056 mmol) was loaded into a Schlenk flask and dissolved in 20 mL of THF. To this solution was added a 20-fold molar excess of NaN_3 (0.08 g, 1 mmol). The pale yellow solution was allowed to stir overnight, turning to an opaque gray by the next day. The solution was evacuated to dryness, dissolved in toluene, and filtered. NMR at this point showed complete conversion. The filtrate, a dark yellow color, was concentrated under vacuum to ∼5 mL and placed into a −40 °C freezer; after two days no crystals were observed. The sample was evacuated to dryness, dissolved in pentane, and filtered. The filtrate was concentrated under vacuum to ∼3 mL and placed into a −40 °C freezer; after two weeks crystals formed. Yield: 0.02 g(66%). The colorless and brown crystals formed were used for X-ray crystallography. ^{1}H NMR (300 MHz, C_6D_6): δ 23.9 (br s, Si−CH_3), 2.61 (br s, ^{t}butyl); CH_2 groups were not observed. IR (pentane solution): 2073 cm^{-1}. MS (positive ion methane CI): (PNP)FeN_3 ($C_{22}H_{52}FeN_4P_2Si_2$), calcd 546.647 g/mol. No parent ion observed apparently because of loss of azide under the energetic conditions.

[(PNP=N)Fe]$_2$. The procedure described for the synthesis of (PNP)FeN_3 was used to synthesize an aliquot of (PNP)FeN_3. After the filtration from the toluene step described above, the sample was evacuated to dryness and dissolved in C_6D_6 and filtered into a J-Young NMR tube. Reference ^{1}H NMR and ^{31}P NMR spectra were taken, and the sample, held at 25 °C, was irradiated using a medium-pressure mercury UV lamp in 10 min intervals, followed by collection of ^{1}H NMR spectra. After the sample had been irradiated for a total of 20 min, ^{1}H NMR showed complete (95%) conversion of (PNP)FeN_3 to product.

The sample was evacuated to dryness and redissolved in pentane. The solution was placed in a vial with a lightly perforated top to allow for slow evaporation of pentane in a glovebox. When slow evaporation proved to be an ineffective means of crystallization, the sample was redissolved in a small quantity of a 9:1 mixture of pentane and toluene and placed into a −40 °C freezer. After two weeks, the sample had formed small crystals, which were used for X-ray data collection. ^{1}H NMR (300 MHz, C_6D_6):6.0 (br s, CH_2), 4.8 (s, Si−CH_3), 3.6 (s, ^{t}butyl), 1.5 (s, CH_2), 1.3 (s, ^{t}butyl), −3.1 (s, Si−CH_3).

The full dimer in the asymmetric unit shows disorder of only one of the pendant phosphine donor arms, in the form of two conformers (populated 82:18) around the N−Si bond. The half-dimer shows no disorder.

(PNP)Fe[NH(xylyl)]. (PNP)FeCl (0.022 g, 0.041 mmol) was added to a J-Young NMR tube and dissolved in C_6D_6, to which was added LiNH(2,6-$Me_2C_6H_3$) (0.006 g, 0.047 mmol). On addition, a slight color change from yellow to brown was observed. The sample was mixed by tumbling overnight. Then, ^{1}H NMR and ^{31}P NMR spectra were taken of the sample, with ^{1}H NMR showing complete conversion and the formation of a paramagnetic product (<90% yield of crude product). The sample was evacuated to dryness, dissolved in pentane, and filtered into a J-Young tube. The filtrate was concentrated to ∼1 mL, and placed into a −40 °C freezer. After one week crystals had formed, and these were used for X-ray structure determination. ^{1}H NMR (300 MHz, C_6D_6): δ 68.4 (br s, CH_3−Ar), 24.1 (br s, P−CH_2−Si), 20.3 (br s, Si−CH_3), 13.8 (br s, H−Ar) 1.60 (br s, ^{t}butyl), −3.41 (br s, H−Ar), −10.6 (br s, H−Ar) −80.1 (br s, CH_3−Ar).

Acknowledgment. This work was supported by the NSF (CHE-0544829). We thank Michael Ingleson for enlightening discussions.

Supporting Information Available: Magnetic susceptibility determinations, graphics of ^{1}H NMR spectra, crystallographic narratives, and full details of the DFT calculations. This material is available free of charge via the Internet at http://pubs.acs.org.

IC702279B

(39) Barrett, A. G. M.; Crimmin, M. R.; Hill, M. S.; Hitchcock, P. B.; Procopiou, P. A. *Angew. Chem., Int. Ed.* **2007**, *46*, 6339.
(40) Kazi, A. B.; Jones, G. D.; Vicic, D. A. *Organometallics* **2005**, *24*, 6051.
(41) Conroy, K. D.; Hayes, P. G.; Piers, W. E.; Parvez, M. *Organometallics* **2007**, *26*, 4464.